JOURNAL OF Applied Polymer SCIENCE

Preparation and properties of a form-stable phase-change hydrogel for thermal energy storage

Tao Wang,[1] Nan Wu,[1] Hui Li,[2] Qu-Liang Lu,[2] Yong Jiang[1]
[1]School of Chemistry and Chemical Engineering, Southeast University, Nanjing, Jiangsu, People's Republic of China 211189
[2]Chengxian College, Southeast University, Nanjing, Jiangsu, People's Republic of China 210088
Correspondence to: Y. Jiang (E-mail: yj@seu.edu.cn)

ABSTRACT: In this study, we aimed to fabricate a form-stable phase-change hydrogel (PCH) with excellent mechanical properties and heat-storage properties. Sodium alginate (SA) and polyacrylamide (PAAm) composite hydrogels were prepared with ionically crosslinked SA in a PAAm hydrogel network. Glauber's salt [i.e., sodium sulfate decahydrate ($Na_2SO_4{\cdot}10H_2O$)] was incorporated within the hydrogel network as a phase-change material. Scanning electron microscopy micrographs revealed that $Na_2SO_4{\cdot}10H_2O$ was confined in the micropores of the hydrogel inner spaces, and differential scanning calorimetry curves showed that the composite hydrogel possessed a considerable storage potential. Mechanical properties tests, such as tensile and compressive measurements, presented a decreasing trend with increasing $Na_2SO_4{\cdot}10H_2O$ dosage. We concluded that the prepared composite PCH could be used to design hydrogel materials with thermal-energy-storage applications. © 2016 Wiley Periodicals, Inc. J. Appl. Polym. Sci. **2016**, *133*, 43836.

KEYWORDS: applications; crosslinking; phase behavior; properties and characterization; thermal properties

Received 21 January 2016; accepted 25 April 2016
DOI: 10.1002/app.43836

INTRODUCTION

The energy crisis, a current severe reality, has captured much attention in recent years. Researchers all over the world are making significant efforts to exploit renewable or new energy resources.[1–3] In this context, the efficient use of energy through the development of novel energy-storage devices can be an alternative for solving both the high consumption of energy resources and greenhouse gas emission issues. One relatively innovative and promising technique is the efficient utilization of latent heat thermal energy storage (LHTES), which has a high storage enthalpy and no apparent temperature change.[4,5] Phase-change materials (PCMs) have been identified to be crucial for LHTES because they are able to store and release a considerable amount of latent heat, that is, the thermal energy from the process of melting and solidification at certain temperatures.[6]

At higher ambient temperatures, PCMs change their phase from solid to liquid within a defined temperature change to store energy and release energy by changing from liquid to solid as the temperature decreases.[7] PCMs are broadly divided into two categories, organic and inorganic materials, according to their composition. A large volume of previous research work has focused on organic PCMs because they have a higher latent heat density, are noncorrosive, perform little or no subcooling, exert good compatibility with most building materials, and have low vapor pressure and stable physical and chemical properties.[8–11] Nevertheless, they also suffer from certain disadvantages, such as a low thermal conductivity, significant changes in volume during repeated phase changes, and flammability.[12] On the other hand, inorganic solid–liquid PCMs have a high latent heat density, excellent thermal conductivity, high enthalpy of fusion, fire resistance, and low cost compared to the organic materials. Inorganic solid–liquid PCMs include salt hydrates, inorganic compounds, metal salts, and eutectics.[13,14] Salt hydrates, such as sodium sulfate decahydrate (SSD or $Na_2SO_4{\cdot}10H_2O$), disodium hydrogen phosphate, and sodium acetate trihydrate, have been studied as PCMs by several authors because of their excellent latent heat-storage capacity.[15–18] Among these, SSD offers maximum cost effectiveness and has thus attracted a lot of attention.[19,20] However, supercooling and incongruent melting are generally prone to generate in inorganic salt hydrates. This signifies that the melt is an oversaturated solution and that phase separation can occur. To reduce supercoiling, heterogeneous nucleation should be taken into account. To initiate the formation of seeds and crystal growth near the freezing temperature, a small amount of a nucleating agent can be added.[21] With respect to phase separation, the viscosity of the salt mixture can be increased by the addition of a thickening agent.[22]

To overcome the defects of inorganic PCMs, which are corrosive to most metals and encounter the phenomena of decomposition

Table I. Formulations for Making PCHs with Different Contents of Na_2SO_4

	Formulation					
	1	2	3	4	5	6
Na_2SO_4 (g)	0	6.76	10.73	15.21	20.28	26.07
H_2O (mL)	43	43	43	43	43	43
Glycerol (mL)	0	1.57	1.57	1.57	1.57	1.57
Borax (g)	0	1.99	1.99	1.99	1.99	1.99
$CaSO_4{\cdot}2H_2O$ (g)	0.166	0.166	0.166	0.166	0.166	0.166
SA (g)	0.625	0.625	0.625	0.625	0.625	0.625
PAAm (g)	0	3	3	3	3	3
AAm (g)	10	10	10	10	10	10
MBA (mg)	15.6	15.6	15.6	15.6	15.6	15.6
Potassium persulfate (mg)	447	447	447	447	447	447
TEMED (mg)	8.1	8.1	8.1	8.1	8.1	8.1
Na_2SO_4 (%)[a]	0	10	15	20	25	30
$Na_2SO_4{\cdot}10H_2O$ (%)[b]	0	23	34	45	56	67

[a] Percentage of the PCM in the form of Na_2SO_4.
[b] Percentage of the PCM in the form of $Na_2SO_4{\cdot}10H_2O$.

and subcooling, an encapsulation strategy is indispensable in a thermal-energy-storage system.[23–27] Most of the current work has been carried out with microencapsulation/nanoencapsulation to form a core–shell structure. Conventional methods, such as *in situ* polymerization, complex coacervation, the sol–gel method, and solvent extraction/evaporation, have been applied extensively in the preparation of a wide range of microspherical products.[28] Nevertheless, most of the core materials have been organic compounds; only a few studies have reported the microencapsulation of salt hydrates. The main problems in the use of traditional microencapsulation/nanoencapsulation technology with salt hydrates are obvious volume changes and the overflow of crystal water into the cavity of the spherical polymer shell material.

A crosslinked three-dimensional polymer network can offer us an alternative method work-around to problems such as phase segregation and supercooling by transforming the structural form of the material system.[29] Three-dimensional crosslinked hydrogels obtained from synthetic and naturally derived polymers exhibit high tensile and compressive strengths, have high permeabilities to small molecules, and undergo reversible volume change by exuding or absorbing water in response to a wide range of stimuli, such as light, temperature, pH, ionic strength, and chemical reactions.[30–32] Sun *et al.*[33] reported a tough and highly stretchable hydrogel, which was developed through the formation of ionically and covalently crosslinked polymer networks.

In this study, we combined the strong mechanical properties of polymer networks and the thermal property advantages of SSD to develop a tough and stretchable hydrogel system in which PCM was incorporated for energy-storage functions. In this study, we fabricated an ionically and covalently crosslinked polymer hydrogel with Glauber's salt to synthesize a phase-change hydrogel (PCH) for thermal energy storage. The obtained PCH was able to maintain a stable form during the thermal-phase-transformation process because of the shape-stabilized hydrogel. The crystal morphology and microstructure of the prepared PCH were observed by polarizing optical microscopy (POM) and scanning electron microscopy (SEM). The thermal and mechanical properties were investigated by differential scanning calorimetry (DSC) and mechanical testing. We also studied the interactions between the polymer network, the effect of PCM on the hydrogel network's mechanical properties, and the influence of the crosslinked hydrogel on the thermal properties of SSD.

EXPERIMENTAL

Materials

Sodium alginate [SA; analytical-reagent (AR) grade], *N,N′*-methylene bisacrylamide (MBA; chemistry pure (CP) grade), and calcium sulfate dihydrate ($CaSO_4{\cdot}2H_2O$; CP grade) were purchased from Aladdin Chemical Reagent Co., Ltd. (Shanghai, China). *N,N,N′,N′*-Tetramethyl ethylene diamine (TEMED; AR grade) was purchased from Sigma Chemical Pty., Ltd. (Perth, Western Australia). Acrylamide (AAm; CP grade), sodium sulfate (Na_2SO_4; industrial product), borax (industrial product), polyacrylamide (PAAm; CP grade), ammonium persulfate (AR grade), and glycerol (Industrial product) were obtained from Sino Pharm Chemical Reagent Co., Ltd. (Shanghai, China). SA, borax, and Na_2SO_4 particles were purified by distillation under reduced pressure before use. The dosages of the reagents are shown in Table I.

Preparation of PCH

SA powder (0.625 g) was dissolved in 43 mL of deionized water at room temperature under stirring for 6 h to form a homogeneous solution. The homogeneous solution was poured into a beaker kept at 50 °C in a thermostatic water bath. To this breaker, we sequentially added 10 g of AAm monomer, Na_2SO_4

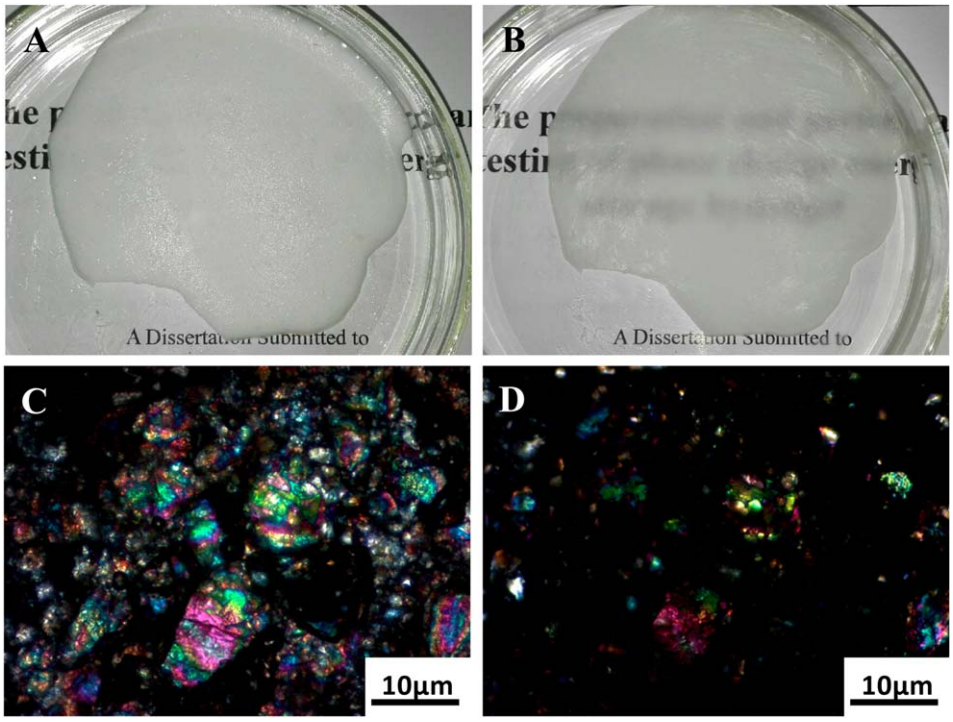

Figure 1. Photographs of a PCH containing 45 wt % $Na_2SO_4{\cdot}10H_2O$ at (A) 10 and (B) 50 °C. POM images of a similar PCH at (C) 10 and (D) 50 °C. [Color figure can be viewed in the online issue, which is available at wileyonlinelibrary.com.]

crystal particles, and 1.987 g of borax (nucleating agent). After stirring this mixture for 20 min, we added 8.1 mg of MBA (crosslinker) and 15.6 mg of TEMED (crosslinking accelerant for PAAm) and stirred it for another 10 min. To this solution, we sequentially added 3.0 g of PAAm powder (thickening agent), 1.5 mL of glycerol solution (humectant), and 0.166 g of a $CaSO_4{\cdot}2H_2O$ slurry as the ionic crosslinker for alginate. Next, 0.0474 g of ammonium persulfate was added as a photoinitiator to initiate the crosslinking reaction of PAAm, and the formative gel was irradiated with ultraviolet light for 2 h (8-W power and 254-nm wavelength at 50 °C). The gel was stored in a humid environment for 24 h to stabilize the reactions, and finally, water from its surface was removed with N_2 gas for 30 s.

POM Measurement

The sample was observed under a polarizing microscope (XPN-300E. Shanghai Changfang Optical Instrument Co., Ltd., China) equipped with a video camera. To observe the crystalline phase of PCH, first we treated the sample with ice. The sample was then placed between a microscopic glass and a cover slip and heated with a hot stage. Then we adjusted the temperature of the hot stage from 5 to 70 °C and observed the POM images.

SEM Measurement

To characterize the morphology of the hydrogel surface, the hydrogels after swelling in water (to an equilibrium state) were fully freeze-dried with a freeze drier (JOYN, FD-1A-50, Shanghai, China) at −52 °C for 24 h. The samples were then examined with an UltraPlus field emission scanning electron microscope (Zeiss, Germany).

DSC Measurements

DSC was performed to analyze the phase-change characteristics of the PCH and the temperature transition of the PCMs in the hydrogel on a DSC-8000 instrument (PerkinElmer). About 5–6 mg of the specimen was put in a hermetically sealed aluminum DSC pan to prevent water loss during scanning. All of the measurements were carried out under a nitrogen atmosphere at a heating or cooling rate of 5 °C/min. The first heating scan was run from 0 to 80 °C, and the specimen was held at this temperature for 5 min to expunge the thermal history before formal measurement.

Measurement of the Subcooling Degree of PCH

To investigate the subcooling degree of the composite hydrogel, we used an electronic digital thermometer with a metal probe, which was inserted inside the hydrogel. The system temperature of the as-prepared hydrogels was about 50 °C. The hydrogels were then placed in a cooler, and measurement was stopped until the hydrogels were cooled to 18 °C. Thereafter, the temperature curves shown by the thermometer (connected to the computer) were considered to be step-cooling curves. The lowest point corresponding to the cooling process in the step-cooling curve and the point corresponding to the platform were called T_1 and T_2, respectively. The subcooling degree was calculated as follows:

$$\text{Subcooling degree} = T_2 - T_1$$

Mechanical Property Tests

Tensile Measurement. We prepared six hydrogels samples by cutting the samples into strips with a length of 25 mm and a width of 5 mm. The thickness was measured by a digital caliper.

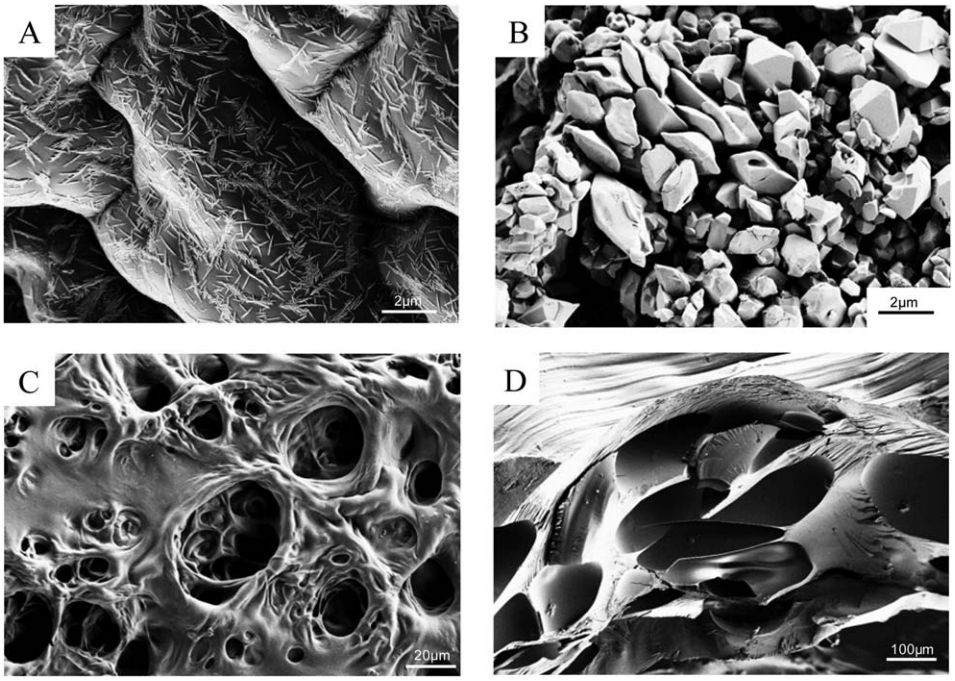

Figure 2. SEM images of different PCHs: (A) surface morphology of PCH containing 45 wt % $Na_2SO_4{\cdot}10H_2O$, (B) cross-sectional image showing the interior morphology of a PCH containing 45 wt % $Na_2SO_4{\cdot}10H_2O$, (C) cross-sectional image showing the microstructure of the aforementioned hydrogel network after Na_2SO_4 was removed from the PCH, and (D) a pure PAAm/SA hydrogel without Na_2SO_4 as a control.

Tensile testing was performed with a YL-1109 tester (Dongguan, China). Tension (newtons) and stretched length (millimeters) were recorded at a speed of 30 min/mm at room temperature. Each sample was tested at least three times. The tensile strength (kPa) of the hydrogels was determined as follows:

$$\text{Tensile strength} = \frac{F}{Wt}$$

$$\text{Elongation (\%)} = \frac{L - L_0}{L_0} \times 100\%$$

where F represents the tension of the samples at break, L represents the elongation of the samples at break, and W, t, and L_0 are the width, height, and length of the samples, respectively.

Compressive Measurement. We prepared six hydrogels samples by cutting cylindrical specimens 20 mm in diameter and 5 mm in height. Compressive testing was also performed with the YL-1109 tester (Dongguan China). The pressure was determined by an instrument at a speed of 5 min/mm at room temperature.

RESULTS AND DISCUSSION

Crystalline Properties of the PCHs

Different PCHs with different percentages of $Na_2SO_4{\cdot}10H_2O$ were prepared with the formulations listed in Table I. The photographs of PCH containing 45 wt % $Na_2SO_4{\cdot}10H_2O$ at different temperatures are shown in Figure 1(A,B). The appearance of the PCH was milky white at 10 °C before phase change, as shown in Figure 1(A). When the temperature was increased to 50 °C, the system turned semitransparent, but it was still in the solid state above the phase-transition temperature [Figure 1(B)]. To reveal the crystalline properties of the PCM in the hydrogel, POM was used to record the crystalline nature of the samples. Figure 1(C) shows the POM images of PCH at 10 °C under polarized light. The colorful area indicates the crystalline phase in the crosslinking network. Next, the sample was heated to 50 °C with a hot stage, and the captured image is shown in Figure 1(D). The colorful area began to fade away and eventually disappeared. These observations confirmed that Na_2SO_4 in the PCH underwent a phase-transition process from the crystalline hydrate phase to the solution phase.

Morphology Characterization of PCH

The microstructures and surfaces of the PCHs were observed with SEM. Figure 2(A) reflects the surface of the PCH that contained SSD. A few flake SSD crystals were found; this demonstrated that most of the salt particles were scattered inside the hydrogel network. To analyze the distribution of the inorganic salt within the hydrogel, a cross section of the hydrogel was observed, and the corresponding micrographs are shown in Figure 2(B). The hydrates were totally embedded in the skeleton of the hydrogel; this allowed the PCMs to undergo the process of phase change.

The same PCH was then immersed in pure water for a long time to remove all of the embedded Na_2SO_4 thoroughly. The internal slices in Figure 2(C) show the inner network structure of PCH. As shown in the images, we clearly observed that a small three-dimensional interspace developed through the crosslinked network in the interior of the hydrogel. The abundant micropores within the gel could house Na_2SO_4 hydrates.

When ambient temperature was lower than the phase-change temperature, water molecules in the hydrogel network

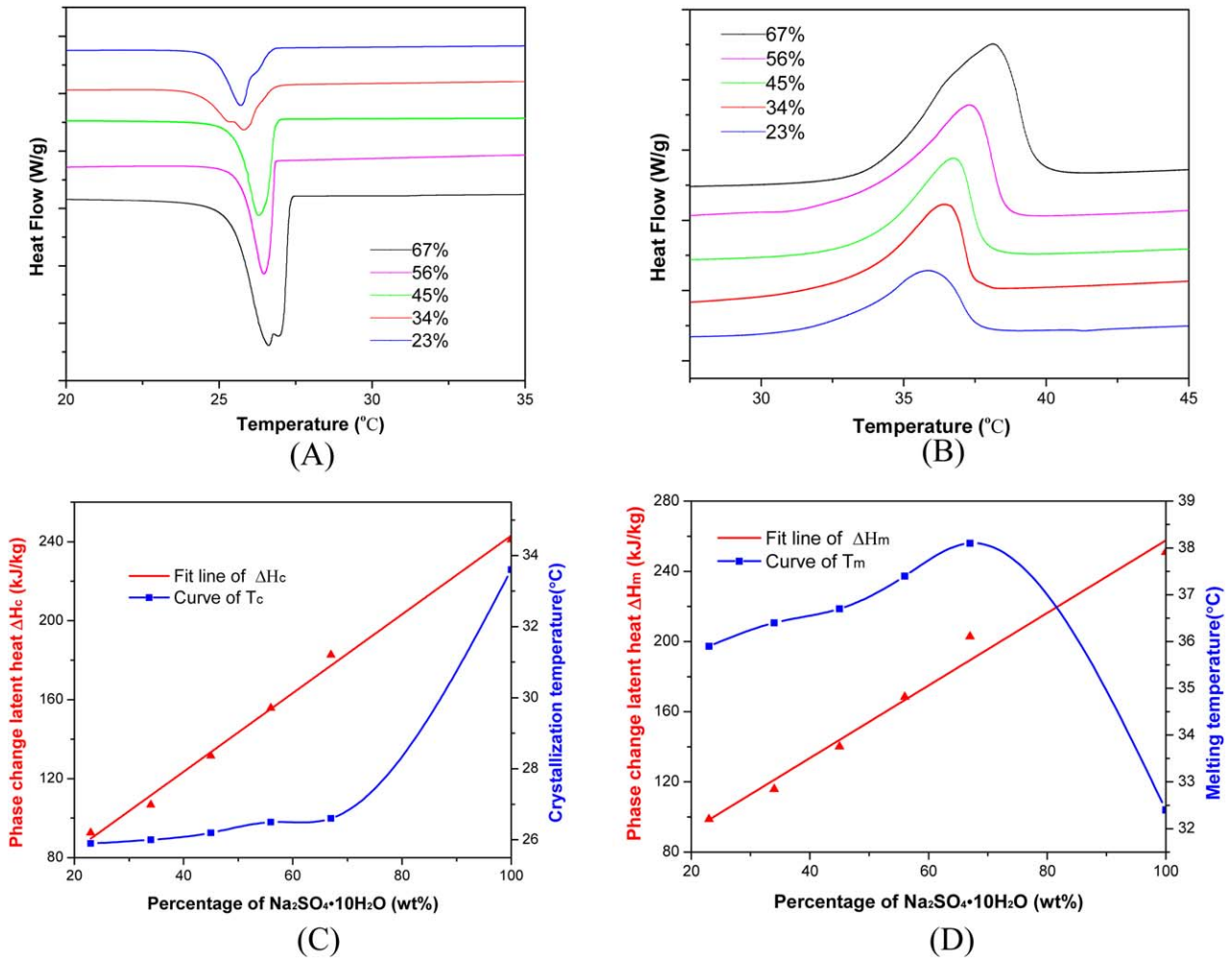

Figure 3. (A,B) DSC curves of cooling and melting, respectively; (C) curves of the crystalline enthalpy (ΔH_c) and crystallization temperature (T_c) with different percentages of $Na_2SO_4{\cdot}10H_2O$; and (D) curves of the melting enthalpy (ΔH_m) and melting temperature (T_m) with different percentages of $Na_2SO_4{\cdot}10H_2O$. [Color figure can be viewed in the online issue, which is available at wileyonlinelibrary.com.]

associated with Na_2SO_4 to produce Na_2SO_4 hydrate. On the other hand, when the ambient temperature was higher than the phase-change point, Glauber's salt released the water of crystallization into the hydrogel again. During this process, in the specified temperature range, the hydrated salt inside the PCHs underwent a phase-change process, and the latent heat was either released or stored to realize energy conversion.

Thermal Properties of PCH

The thermal properties played a critical role in the investigation of the performance of PCH when applied to thermal regulation, especially for the energy-storage system. As shown in Figure 3(A,B), DSC analysis revealed the phase-change temperature, the theoretical enthalpies, and the latent heats. The obtained phase change, latent heat, and crystallization temperature with DSC are listed in Table II.

From the previous experimental data, sharp peaks were observed; these indicated a solid–liquid phase change of Glauber's salt within the hydrogels. Interestingly, as shown in Figure 3(A), the crystallization peak for the 67 wt % specimen exhibited an inconspicuous bimodal crystallization behavior in the DSC cooling thermograms. However, only a single endothermic peak was observed in the melting process, as shown in Figure 3(B). It was reported earlier that under some conditions, Na_2SO_4 displayed a metastable phase transformation to $Na_2SO_4{\cdot}7H_2O$ with a transformation temperature above the bulk crystallization temperature before it was completely converted to $Na_2SO_4{\cdot}10H_2O$ crystals.[34] In this case, the 67 wt % specimen exhibited two phase-transformation temperatures, which could be assigned to the transitions from the homogeneously nucleated liquid to a rotator phase and then from the heterogeneously nucleated rotator phase to a crystalline phase in the cooling process.[35] Such characteristics led to the two-peak structure of the DSC cooling curves because of two phase transitions; this originated because of insufficient free water in the hydrogel network. On the other hand, the single melting peak of the 67 wt % specimen shown in Figure 3(B) was attributed to the phase transition from the monoclinic crystal phase to a liquid phase in the heating process. Figure 3(C,D) shows that the crystalline and melting enthalpies of PCH had an increasing trend with increasing amount of $Na_2SO_4{\cdot}10H_2O$. The maximum latent heats of the prepared PCHs reached 182.7 and 202.9 kJ/kg in the cooling and heating

Table II. Thermal-Energy-Storage Properties of the $Na_2SO_4·10H_2O$ and PAAm/SA Composite Hydrogels

	Formulation					
	1	2	3	4	5	6
$Na_2SO_4·10H_2O$ (%)	23	34	45	56	67	100
ΔH_c (kJ/kg)[a]	92.6	106.7	131.5	155.8	182.7	241
T_c (°C)[b]	25.9	26.0	26.2	26.5	26.6	33.6
ΔH_m (kJ/kg)[c]	98.8	115.9	140.12	168.44	202.9	251
T_m (°C)[d]	35.9	36.4	36.7	37.4	38.1	32.4

[a] Phase-change latent heat of crystallization.
[b] Crystallization temperature.
[c] Phase-change latent heat of melting.
[d] Melting temperature.

processes, respectively, with the 67 wt % $Na_2SO_4·10H_2O$. When more $Na_2SO_4·10H_2O$ was added to the hydrogel, the excess salt precipitated to the bottom of hydrogel, even though additional PAAm powder was added to prevent phase separation. The thermal properties of the pure $Na_2SO_4·10H_2O$, as reported in the literature, are also listed in Table II.[36,37] The latent heat of crystalline enthalpy values fitted a linearly increasing curve very well, as shown in Figure 3(C); this signified that the decrease in the enthalpies in the PCHs was mainly due to the decrease in the percentage $Na_2SO_4·10H_2O$. With respect to the melting enthalpy values shown in Figure 3(D), this linear trend was not evident.

The crystallization temperature of the PCHs was lower than that of pure $Na_2SO_4·10H_2O$, whereas the melting temperature seemed to have an opposite tendency. The difference was possibly due to the diminution of the thermosensitivity of the PCMs because of shielding by the crosslinking hydrogel network, and finally, this caused hysteresis of phase transformation. According to the Gibbs–Thomson equation, the phase-change temperature is influenced by porous media.[38] Furthermore, a decrease-in-the-freezing-point principle could also help explain the decrease in the hydrate phase-change temperature due to the addition of PCM. In another perspective, because the experimental phase temperature was within the range of human comfort, the hydrogel system could be applied to building materials to stabilize fluctuations in indoor temperature or in seat cushions.

Effect of the $Na_2SO_4·10H_2O$ Content on the Subcooling Degree of the PCH System

Subcooling is one of the main defects that PCMs need to overcome. As shown in Figure 4, the subcooling of the pure $Na_2SO_4·10H_2O$ was up to 10 °C. We could solve this problem quite well by embedding $Na_2SO_4·10H_2O$ into the hydrogel network. Within a certain range, the system's subcooling degree gradually decreased to 0 °C with the improvement of the $Na_2SO_4·10H_2O$ content. However, when the content exceeded a certain limit, the subcooling degree augmented sharply. The reason could be explained like this: inorganic particles began to aggregate massively in the network, whereas the $Na_2SO_4·10H_2O$ increased to a specific extent. Under this circumstance, the nucleating agent could not play a significant role of inhibition for reducing the subcooling degree; in the meantime, we observed small inorganic particles precipitating at the bottom of reaction vessel. Consequently, we drew the conclusion that the structure of the multiple crosslinking network effectively prevented PCH subcooling with the appropriate $Na_2SO_4·10H_2O$ content.

Mechanical Properties of the Composite PCHs

The mechanical properties of the prepared PCHs were important parameters for their use as load-bearing materials. The prepared PCHs were excellent in strength and relatively tough during the process of stretching. As shown in Figure 5(A,B), the PCHs had an excellent tensile strength due to the length extension reached, approximately 17 times, and it hardly snapped during the tensile fracture process. From the further evidence provided in Figure 5(C), this illustrated the tensile properties for the composite PCH with $Na_2SO_4·10H_2O$ contents ranging from 0 to 67 wt %. When we exerted tensile strain on the prepared samples that had no inorganic salts, the fracture strength reached above 130 KPa. Meanwhile under tensile strain, they sustained elongations up to 1500% or even higher before fracture. With increasing $Na_2SO_4·10H_2O$ content, the tensile strength and elongation gradually presented a decreasing trend. Although the elastic modulus was influenced by the dosage of $Na_2SO_4·10H_2O$, it still acquired a considerable quantitative value, which was appropriate for application.

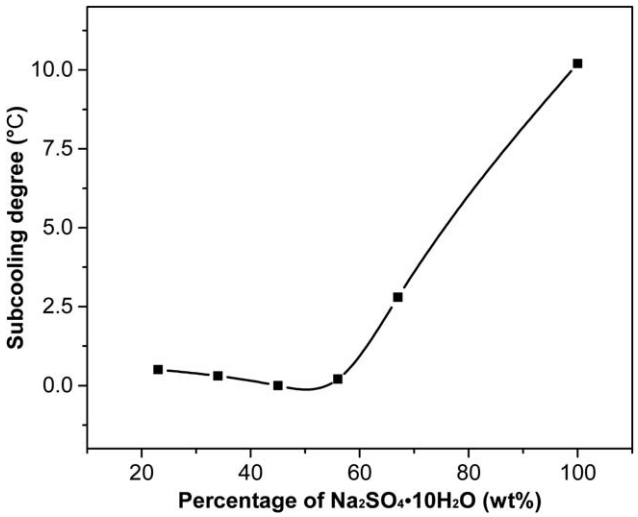

Figure 4. Relationship between the subcooling degree and various $Na_2SO_4·10H_2O$ contents.

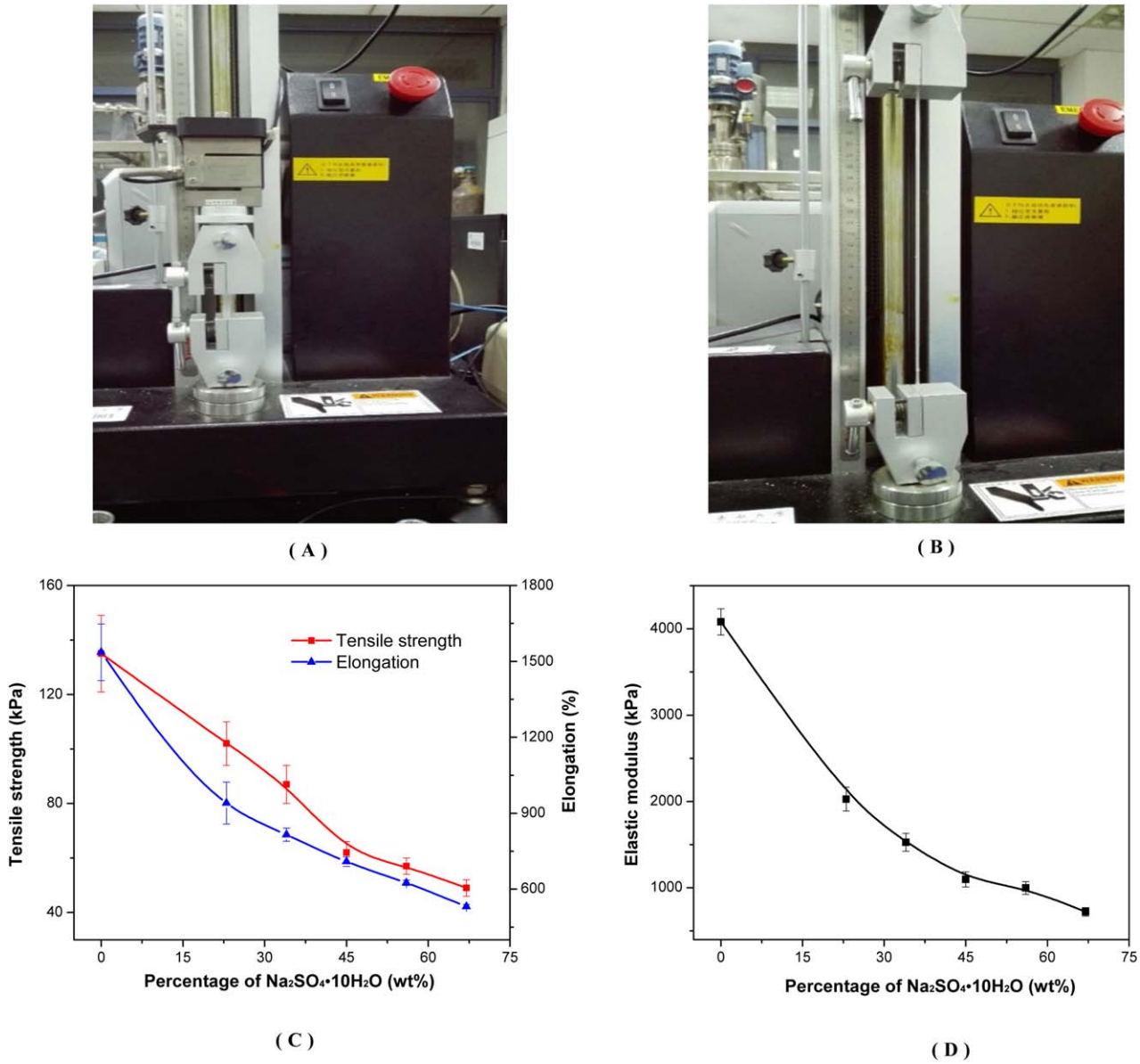

Figure 5. Mechanical property test of PCHs with various $Na_2SO_4{\cdot}10H_2O$ percentages: (A) before stretch, (B) after stretch, (C) tensile properties of the composite hydrogels, and (D) compressive properties of the composite hydrogels. [Color figure can be viewed in the online issue, which is available at wileyonlinelibrary.com.]

Generally, a higher and excellent mechanical strength is caused by a denser network.[39] The experiment performed here also showed a similar result. The proposed factors that contributed to the hydrogel strength are discussed as follows. The strength of the hydrogels was influenced by the incorporated PCM particles because the free volume of the inner network in the hydrogel decreased. As a result, the material became less rigid; this resulted in a reduction in the elastic modulus. Moreover, because of the incorporation of the PCM, the polymer chain movement space was blocked, and the movement of the polymer chains were restricted. When the hydrogel was stretched, the chain segment network partly ruptured because of the brittleness of the salt stored between the crack tips.

The compression modulus, characterized by the elastic modulus, is also the essential index for the evaluation of a material's stiffness when used as cushion material. From the analysis in Figure 5(D), we observed a steady decrease in the elastic modulus for the composite hydrogels with increasing dosage of PCM. Figures 4 and 5 confirm that the lower mechanical properties caused by the increase in the $Na_2SO_4{\cdot}10H_2O$ content signified a looser crosslinking density. This indicated that the material became more frangible, and this resulted in a decrease in the elastic modulus.

Both the mechanical properties and thermal properties of PCH were affected by the content of $Na_2SO_4{\cdot}10H_2O$ in the hydrogel. The volume occupied by the salt hydrates in the hydrogel network was oppositely related to the mechanical properties of the hydrogel. However, when larger amounts of PCM particles ($Na_2SO_4{\cdot}10H_2O$) were incorporated into the hydrogel, more improved thermal properties were achieved. Thus a reverse

trend was observed between the mechanical and thermal properties of the hydrogel, both of which played a vital role in practical applications. Primarily, there were two limitations in the efficient utilization of the hydrogels as LHTES materials:

1. The enthalpy of PCH could not be released or absorbed exhaustively because of the crosslinked hydrogel network. This caused obstruction, and it became difficult for the free water to integrate with Na_2SO_4. This implied that the energy-storage efficiency was not so high.
2. Because of the presence of inorganic salts, the strength of the material was not so considerable but still had some practical limits.

CONCLUSIONS

To conclude, a novel PCH was fabricated for latent heat-storage application by the incorporation of Na_2SO_4 hydrates into the microspace formed by a multiple crosslinking hydrogel network through *in situ* free-radical polymerization. The maximum percentage of $Na_2SO_4{\cdot}10H_2O$ contained within the hydrogel network without leakage was 67%. POM images showed that the phase transition of the inorganic salt was formed, Na_2SO_4 to $Na_2SO_4{\cdot}10H_2O$; this was achieved by bonding with the free water within the hydrogel network. SEM micrographs showed that $Na_2SO_4{\cdot}10H_2O$ was spread around the pores within the inner spaces of the hydrogel. The phase-change temperature of the composite hydrogels was in the proper range of human comfort, and it also presented considerable energy-storage potential, as shown by the DSC curves. The mechanical properties tests, including tensile and compressive measurements, presented a decreasing trend with increasing Na_2SO_4 dosage. However, the mechanical properties of these composites were still acceptable for load-bearing materials. Compared to the pure hydrated salts and hydrogels without PCMs, which were made by the PAAm network, the PCHs combined the thermal properties of $Na_2SO_4{\cdot}10H_2O$ and the mechanical properties of PAAm hydrogels. Therefore, the prepared composite hydrogels containing PCM are promising candidates for the applications of LHTES. The raw materials for the preparation of PCH are easy to obtain, and most of them have a low cost. Furthermore, the whole preparation technique can be tailored and is energy-efficient. These facts indicate the economic viability of the prepared materials. The application of these PCHs as energy-storage materials should result in improvements in the efficiency of energy resources. These materials may also be suitable for the energy consumption of buildings.

ACKNOWLEDGMENTS

This work was supported by the National Natural Science Foundation of China (contract grant number 21174029), the Industry Academia Cooperation Innovation Fund of Jiangsu Province (contract grant number BY2014127-07), and the Project Funded by the Priority Academic Program Development of Jiangsu Higher Education Institutions.

REFERENCES

1. Memon, S. A.; Lo, T. Y.; Barbhuiya, S. A.; Xu, W. *Energy Buildings* **2013**, *62*, 360.
2. Sharma, A.; Tyagi, V. V.; Chen, C. R.; Buddhi, D. *Renewable Sustainable Energy Rev.* **2009**, *13*, 318.
3. Su, W.; Darkwa, J.; Kokogiannakis, G. *Renewable Sustainable Energy Rev.* **2015**, *48*, 373.
4. Mehrali, M.; Latibari, S. T.; Mehrali, M.; Mahlia, T. M. I.; Metselaar, H. S. C. *Energy Conversion Manage.* **2014**, *88*, 206.
5. Rathod, M. K.; Banerjee, J. *Renewable Sustainable Energy Rev.* **2013**, *18*, 246.
6. Mehrali, M.; Latibari, S. T.; Mehrali, M.; Mahlia, T. M. I.; Sadeghinezhad, E.; Metselaar, H. S. C. *Appl. Energy* **2014**, *135*, 339.
7. Memon, S. A.; Lo, T. Y.; Cui, H.; Barbhuiya, S. *Energy Buildings* **2013**, *66*, 697.
8. Mahmoud, S.; Tang, A.; Toh, C.; Al-Dadah, R.; Soo, S. L. *Appl. Energy* **2013**, *112*, 1349.
9. Pielichowska, K.; Pielichowski, K. *Prog. Mater. Sci.* **2014**, *65*, 67.
10. Reddigari, M. R.; Nallusamy, N.; Bappala, A. P.; Konireddy, H. R. *Therm. Sci.* **2012**, *16*, 1097.
11. Zhao, C. Y.; Lu, W.; Tian, Y. *Sol. Energy* **2010**, *84*, 1402.
12. Baetens, R.; Jelle, B. P.; Gustavsen, A. *Energy Buildings* **2010**, *42*, 1361.
13. Cabeza, L. F.; Castell, A.; Barreneche, C.; de Gracia, A.; Fernandez, A. I. *Renewable Sustainable Energy Rev.* **2011**, *15*, 1675.
14. Zhao, C. Y.; Zhang, G. H. *Renewable Sustainable Energy Rev.* **2011**, *15*, 3813.
15. Lan, X. Z.; Tan, Z.-C.; Shi, Q.; Yang, C. G. *Thermochim. Acta* **2007**, *463*, 18.
16. Magin, R. L.; Mangum, B. W.; Statler, J. A.; Thornton, D. D. *J. Res. Natl. Bur. Stand.* **1981**, *86*, 181.
17. Naumann, R.; Emons, H. H. *J. Therm. Anal.* **1989**, *35*, 1009.
18. Wada, T.; Matsunaga, K.; Matsuo, Y. *Bull. Chem. Soc. Jpn.* **1984**, *57*, 557.
19. Brown, P. W.; Grimes, J. W.; Kaetzel, L. *Sol. Energy Mater.* **1986**, *13*, 453.
20. Marliacy, P.; Solimando, R.; Bouroukba, M.; Schuffenecker, L. *Thermochim. Acta* **2000**, *344*, 85.
21. Cabeza, L. F.; Svensson, G.; Hiebler, S.; Mehling, H. *Appl. Therm. Eng.* **2003**, *23*, 1697.
22. Waqas, A.; Din, Z. U. *Renewable Sustainable Energy Rev.* **2013**, *18*, 607.
23. Chen, L.; Xu, L.; Shang, H.; Zhang, Z. *Energy Conversion Manage.* **2009**, *50*, 723.
24. Fang, G.; Li, H.; Yang, F.; Liu, X.; Wu, S. *Chem. Eng. J.* **2009**, *153*, 217.
25. Jin, Z.; Wang, Y.; Liu, J.; Yang, Z. *Polymer* **2008**, *49*, 2903.
26. Li, W.; Zhang, X.-X.; Wang, X.-C.; Niu, J.-J. *Mater. Chem. Phys.* **2007**, *106*, 437.

27. Zhang, H.; Wang, X. *Sol. Energy Mater. Sol. Cells* **2009**, *93*, 1366.
28. Salaun, F.; Devaux, E.; Bourbigot, S.; Rumeau, P. *Carbohydr. Polym.* **2010**, *79*, 964.
29. Parke-Houben, R.; Fox, C. H.; Zheng, L. L.; Waters, D. J.; Cochran, J. R.; Ta, C. N.; Frank, C. W. *J. Mater. Sci. Mater. Med.* **2015**, *26*, 107.
30. Chen, Y. M.; Shiraishi, N.; Satokawa, H.; Kakugo, A.; Narita, T.; Gong, J. P.; Osada, Y.; Yamamoto, K.; Ando, J. *Biomaterials* **2005**, *26*, 4588.
31. Gong, J. P. *Soft Matter* **2010**, *6*, 2583.
32. Kwon, H. J.; Yasuda, K.; Ohmiya, Y.; Honma, K.-I.; Chen, Y. M.; Gong, J. P. *Acta Biomater.* **2010**, *6*, 494.
33. Sun, J.-Y.; Zhao, X.; Illeperuma, W. R. K.; Chaudhuri, O.; Oh, K. H.; Mooney, D. J.; Vlassak, J. J.; Suo, Z. *Nature* **2012**, *489*, 133.
34. Rodriguez-Navarro, C.; Doehne, E.; Sebastian, E. *Cem. Concr. Res.* **2000**, *30*, 1527.
35. Genkinger, S.; Putnis, A. *Environ. Geol.* **2007**, *52*, 295.
36. Donkers, P. A. J.; Linnow, K.; Pel, L.; Steiger, M.; Adan, O. C. G. *Chem. Eng. Sci.* **2015**, *134*, 360.
37. Kenisarin, M.; Mahkamov, K. *Sol. Energy Mater. Sol. Cells* **2016**, *145*, 255.
38. Zhang, D.; Tian, S.; Xiao, D. *Sol. Energy* **2007**, *81*, 653.
39. Wang, Q.; Hou, R.; Cheng, Y.; Fu, J. *Soft Matter* **2012**, *8*, 6048.